Nonequilibrium optical-phonon population by sequential resonant tunneling in GaAs-AlAs superlattices

S. H. Kwok and M. Ramsteiner
Paul-Drude-Institut für Festkörperelektronik, Hausvogteiplatz 5-7, D-10117 Berlin, Germany

D. Bertram
Max-Planck-Institut für Festkörperforschung, Heisenbergstrasse 1, D-70569 Stuttgart, Germany

M. Asche
Paul-Drude-Institut für Festkörperelektronik, Hausvogteiplatz 5-7, D-10177 Berlin, Germany

H. T. Grahn
Paul-Drude-Institut für Festkörperelektronik, Hausvogteiplatz 5-7, D-10177 Berlin, Germany
and Research Center for Quantum Effect Electronics, Tokyo Institute of Technology, 2-12-1 O-okayama, Meguro-ku, Tokyo 152, Japan

K. Ploog
Paul-Drude-Institut für Festkörperelektronik, Hausvogteiplatz 5-7, D-10177 Berlin, Germany
(Received 4 October 1995)

We report on the observation of nonequilibrium GaAs LO phonons generated by the relaxation of hot electrons due to sequential resonant tunneling in strongly coupled superlattices. Raman-scattering experiments were performed at 5 K with low optical excitation density. The anti-Stokes LO-phonon intensity, which gives a measure of the nonequilibrium LO-phonon population, exhibits maxima at the resonant tunneling voltages. The transport data show that the electrical heating power increases linearly with voltage. Our results suggest that hot-electron cooling via acoustical phonon emission is suppressed under sequential resonant tunneling conditions.

In semiconductor superlattices (SL's), additional channels for electron transport exist due to miniband formation.[1] For large electric fields along the growth direction, conduction can occur via tunneling from the first subband in one well to a higher subband in the neighboring well.[2] The conduction is strongly enhanced when the ground and adjacent wells are aligned under the applied bias. This is also true when the transition between these states is phonon assisted. The energy, which the electrons acquire by tunneling into the neighboring well, is dissipated by phonon emission. If the carrier energy is higher than the energy of an optical phonon ($\hbar\omega_{\mathrm{LO}}$), the most effective way of relaxation is via emission of LO phonons. For such hot electrons, this dissipation process is up to two orders of magnitude stronger than the relaxation by acoustical phonons, which dominates otherwise. Therefore, transport across the barriers with subsequent emission of optical phonons by intersubband and intrasubband scattering builds up a large nonequilibrium population of LO phonons. Phonon-assisted tunneling also contributes to the nonequilibrium population. The reabsorption of LO phonons[3,4] can change the electron relaxation time and the transport properties of the SL.

The vertical transport properties of carriers in semiconductor superlattices are of great current interest. Although the actual course of carrier cooling can affect the fundamental electronic properties of superlattices, a direct experimental study of nonequilibrium phonons generated by carrier relaxation during vertical transport has not been performed so far. In this work we report on a Raman scattering study of nonequilibrium GaAs LO phonons generated by the relaxation of hot electrons due to sequential resonant tunneling (SRT) in strongly coupled superlattices. Previous Raman investigations focused on the nonequilibrium phonon population generated by the relaxation of photoexcited hot carriers.[5–12] For nonresonant Raman studies of a system at thermal equilibrium, the ratio of the anti-Stokes $[I_{\mathrm{AS}}(\omega_i=\omega-\omega_{\mathrm{LO}}, \omega_s=\omega)]$ and Stokes $[I_S(\omega_i=\omega,\omega_s=\omega-\omega_{\mathrm{LO}})]$ intensities is approximately equal to the ratio $N/(N+1)$,where ω_i and ω_s stand for the excitation and scattering frequency, respectively. N is the Bose-Einstein occupation factor. At 5 K, the anti-Stokes to Stokes ratio is extremely small ($\sim 10^{-37}$). The situation is more complicated for resonant Raman scattering because the resonant conditions for Stokes and anti-Stokes scattering are not the same.[9,10] At helium temperature, the anti-Stokes Raman intensity is proportional to the number of the nonequilibrium LO phonons in the wells. The correlation between the field dependence of nonequilibrium LO-phonon population and the tunneling resonance can be investigated by comparing the Raman and transport measurements for the same sample.

The investigated SL structures are grown by molecular beam epitaxy along the $\langle 001\rangle$ direction. The SL's are embedded in p-i-n structures. The p and n regions consist of highly doped $Al_{0.5}Ga_{0.5}As$ layers. Three samples are studied and their parameters are listed in Table I. The diodes are etched into mesas of 120 μm diameter with Ohmic contacts of Cr-Au on the top and AuGe-Ni on the substrate side. The built-in voltage of the samples is 1.5 V. All measurements are

TABLE I. Parameters, calculated subband spacings, and calculated resonance voltages for *p-i-n* structures for the investigated GaAs-AlAs superlattices.

Sample No.	well width (nm)	barrier width (nm)	No. of periods	involved subbands	spacings (meV)	applied voltages (V)
1	27.0	1.7	40	E_2-E_1	20	0.7
				E_3-E_1	53	-0.6
				E_4-E_1	99	-2.5
				E_5-E_1	159	-4.9
2	18.3	1.4	50	E_2-E_1	40	-0.5
				E_3-E_1	108	-3.9
				E_4-E_1	202	-8.6
3	11.3	1.7	50	E_2-E_1	94	-3.2
				$E_2-E_1+\hbar\omega_{\mathrm{LO}}^{\mathrm{GaAs}}$	130	-5.0
				$E_2-E_1+\hbar\omega_{\mathrm{LO}}^{\mathrm{AlAs}}$	144	-5.7

performed at temperatures below 10 K. The Raman spectra are obtained using the 647.1-nm and 676.4-nm Kr^+-ion laser lines and the 632.8-nm line of a He-Ne laser. The scattering configuration is $z(x',x')\bar{z}$, where x' and z denote $\langle 110\rangle$ and $\langle 001\rangle$ directions, respectively. From the scattering geometry, the nominal in-plane wave vectors of LO phonons observed in Raman scattering are about 2×10^4 cm^{-1}. Typical excitation densities are 25–75 W cm^{-2}, which is very low compared to the previous Raman studies on hot phonons. Time-of-flight measurements are employed to study the approximate transit time of electrons. The details of this technique are given in Refs. 13 and 14. In Table I, E_i-E_1 is the separation between C_i and C_1, where C_i denotes the ith conduction subband. The subband spacings in the table are calculated at zero electric field.

In Fig. 1, typical low-temperature Stokes and anti-Stokes Raman spectra of sample 1 at -6 V are shown. The anti-Stokes LO-phonon intensity is only about 100 times weaker than the Stokes intensity. This is unexpectedly high for a temperature as low as 5 K. We qualitatively determine the relative change of the hot phonon population from the voltage dependence of the anti-Stokes line. We do not attempt to analyze our data quantitatively because of the complex field dependences of Stokes and anti-Stokes resonance profiles.[15] In Fig. 2, we plot the anti-Stokes Raman intensity versus voltage in sample 1. First, the signal only appears above the $C_1\rightarrow C_3$ resonant tunneling voltage (-1.8 V). Second, the most striking point of the data is that the anti-Stokes intensity peaks at about -3 and -5.5 V. Time-of-flight measurements show that the transit time of electrons exhibits minima at the above voltages. According to the calculated subband spacings, these voltages correspond to $C_1\rightarrow C_4$ and $C_1\rightarrow C_5$ tunneling resonances, respectively (cf. Table I). The small shifts between the measured resonant voltages and the calculated values are probably due to the screening effect and the change of Raman efficiency with voltage. Our results suggest that the nonequilibrium LO-phonon population exhibits maxima at the SRT voltages. Due to the resonant effect in the Raman scattering efficiency, the peak intensity depends very much on the excitation wavelength. However, the voltage positions of the peaks do not vary much with the

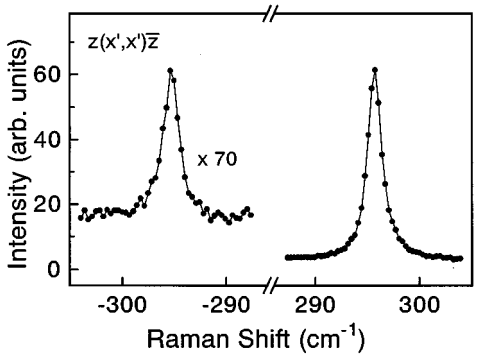

FIG. 1. Typical Stokes and anti-Stokes Raman spectra of sample 1 at 5 K for an applied voltage of -6 V using an excitation density of 37 W cm^{-2} at 632.8 nm.

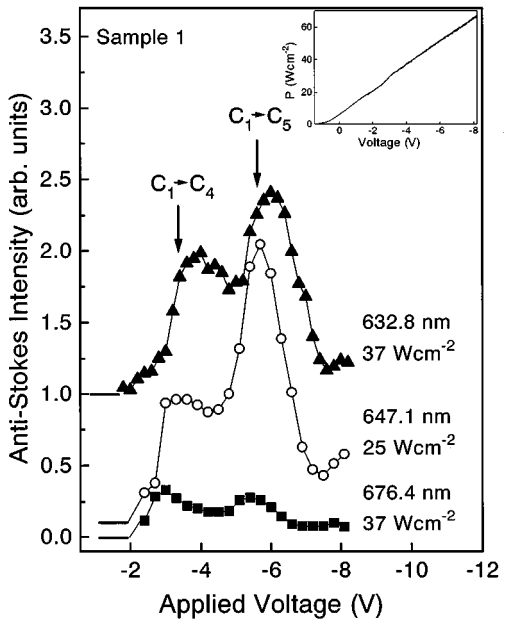

FIG. 2. Voltage dependence of anti-Stokes LO-phonon intensity of sample 1 at 5 K. The arrows label the $C_1\rightarrow C_4$ and $C_1\rightarrow C_5$ tunneling resonances. Three excitation wavelengths are used. Inset: Voltage dependence of the electrical power input of the same sample using an excitation density of 37 W cm^{-2} at 632.8 nm.

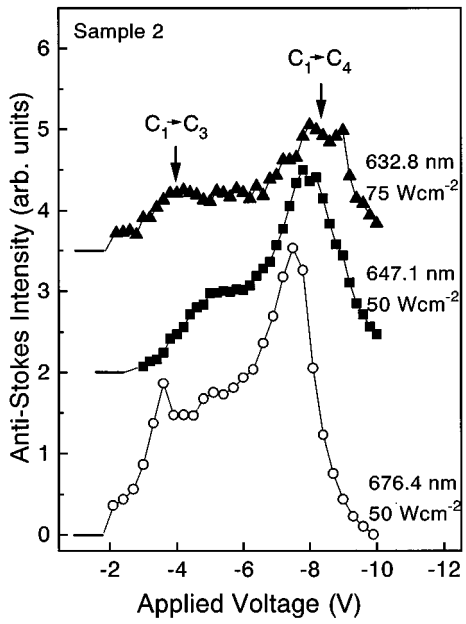

FIG. 3. Voltage dependence of the anti-Stokes LO-phonon intensity of sample 2 at 5 K. The arrows label the $C_1 \rightarrow C_3$ and $C_1 \rightarrow C_4$ tunneling resonances. Three excitation wavelengths are used.

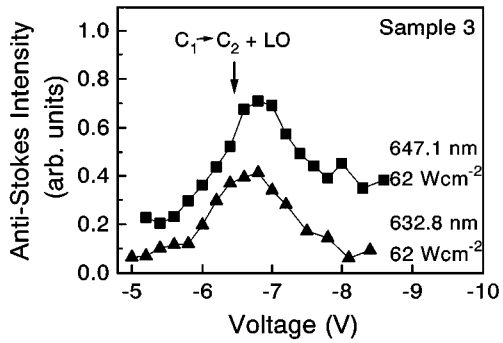

FIG. 4. Voltage dependence of the anti-Stokes LO-phonon intensity of sample 3 at 5 K. The Raman signal peaks at the voltage where $C_1 \rightarrow C_2$+LO resonant tunneling occurs. Two excitation wavelengths are used.

excitation wavelength (cf. Fig. 2), which demonstrates that these features are related to resonant tunneling. In contrast, the field dependence of the Stokes intensity does not show any correlation with transport. The inset of Fig. 2 displays the voltage dependence of the electrical power input to the sample (P) as calculated from the static current-voltage (I-V) characteristic under photoexcitation. P increases almost linearly with voltage. Since in our strongly coupled SL's all the photoexcited electrons can reach the contacts before they can recombine with holes, the current saturates at rather low voltage (about -2 V). The heating electrical power should be equal to the power dissipated via emission of phonons. The different behavior of the LO-phonon population and the electrical power input is rather unexpected.

In sample 2, the $C_1 \rightarrow C_3$ and $C_1 \rightarrow C_4$ tunneling resonances occur at -4 and -9 V, respectively, as calculated from the subband spacings. Figure 3 illustrates the voltage dependence of the anti-Stokes intensity for this sample. The intensity increases from zero when the bias voltage is above the $C_1 \rightarrow C_2$ resonance. Again it clearly shows that the nonequilibrium LO phonon population peaks near the voltages for which the $C_1 \rightarrow C_3$ and $C_1 \rightarrow C_4$ resonant tunneling conditions are satisfied (cf. Table I).

In sample 3, we observe a nonzero anti-Stokes intensity below -5 V. However, the ratio of anti-Stokes to Stokes intensity is about 3 to 5 times smaller compared to the other two samples. This is reasonable because the numbers of photons absorbed and photoexcited carriers per well are smaller for samples with narrower wells. Figure 4 illustrates the change of anti-Stokes intensity versus voltage for sample 3. No measurable signal was observed for excitation at $\lambda = 676.4$ nm. The intensity exhibits a peak at the voltage for which the tunneling resonance assisted by the emission of a GaAs LO phonon is expected.[16,17] Previous transport studies suggest that a strong $C_1 \rightarrow C_2$+LO tunneling resonance occurs at -6.2 V in this sample,[17] which differs from the calculated value (-5.0 V). The LO phonons emitted during phonon-assisted tunneling would contribute to the nonequilibrium LO-phonon population. In both samples 2 and 3, the current becomes almost constant for voltages below -2 and -4 V, respectively. Therefore, the electrical heating effect exhibits a linear dependence at higher voltages.

In principle, Raman backscattering only probes the excitation with in-plane wave vectors less than 10^5 cm^{-1} in a GaAs quantum well system. The wave vectors (Q) of nonequilibrium LO phonons generated by the intrasubband relaxation of hot electrons are in the range of 10^5–10^6 cm^{-1}. Therefore, these nonequilibrium LO phonons should not be observable for perfect samples. LO phonons with Q less than 10^5 cm^{-1} can be produced by intersubband relaxation of hot carriers if the subband spacing is approximately equal to the LO-phonon energy of 36.5 meV.[18] The wave vectors of the LO phonons emitted during phonon-assisted resonant tunneling are also small. However, earlier Raman studies suggested that the phonons with large in-plane Q ($>10^5$ cm^{-1}) are also Raman active under resonant excitation conditions.[19–21] This was attributed to the effect of interface roughness.

If the electrical energy is totally dissipated by LO-phonon emission, one would expect that the field dependence of the electrical and Raman measurements should be similar. However, the electrical data do not show any significant nonlinear structure. This unexpected behavior can only be explained by assuming that a significant amount of the hot electrons lose energy by acoustical-phonon emission. In principle, the hot electron relaxation can proceed by emission of LO and acoustical phonons. From energy conservation, the total heating electrical power (P) is equal to the sum of the energies dissipated by acoustical- and optical-phonon emission. The heating effect due to photoexcitation is small when we compare the energy of hot electrons gained by photoexcitation and SRT. The acoustical-phonon-emission term is only important for those electrons with excess energies smaller than $\hbar\omega_{\mathrm{LO}}$. Although the typical acoustical-phonon-scattering rate is relatively slow,[8,22] the energy dissipation by acoustical-phonon emission is not negligible since most of the electrons occupy the first subband. In our samples, the typical transit time per period lies below 100 ps for voltages below -2 V. This value is only one to two orders of magnitude larger than the typical LO relaxation time. Conse-

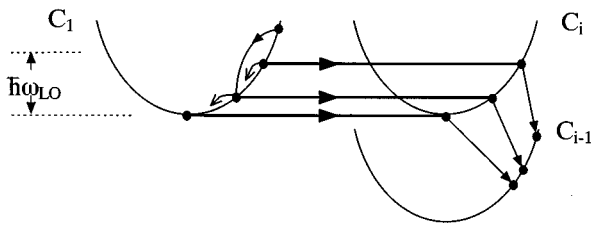

FIG. 5. (a) Schematic diagrams illustrating two neighboring wells at $C_1 \rightarrow C_i$ resonant tunneling voltage. Various paths of hot electron cooling before and after tunneling are shown. Intersubband relaxation from $C_i \rightarrow C_{i-1}$ occurs via LO-phonon emission. For electrons in C_1 with energies smaller than $\hbar\omega_{\mathrm{LO}}$, usually only cooling via emission of acoustical phonons is possible. Under resonant tunneling condition, most of these electrons tunnel into the adjacent well before acoustical-phonon emission occurs.

quently, a large population of nonequilibrium phonons is present. Figure 5 shows a schematic diagram of tunneling and relaxation of electrons at a resonant tunneling voltage. A simple cascade relaxation picture is assumed. We estimate that the typical two-dimensional carrier density within each quantum well is about 10^{10} cm^{-2}. Despite the strong coupling among the wells, the hot electron concentration in the higher subbands is less than 10^{9} cm^{-2}. Therefore, the phonon reabsorption and electron-electron scattering are neglected.[3,23] Since the well-to-well transit time is comparable to the acoustical-phonon-scattering time, a significant population of hot electrons with energies smaller than $\hbar\omega_{\mathrm{LO}}$ exists in the first subband. Under SRT condition, these hot electrons can tunnel into the adjacent well within a fraction of the relaxation time for acoustical-phonon emission because the transport time is drastically reduced. Thus, the process of acoustical-phonon emission is not very likely to be completed. However, the cooling process via LO-phonon emission is not affected by vertical transport due to the extremely short LO-phonon scattering time ($\sim$ 0.1 ps). As a result, the probability per unit time for LO-phonon emission is dramatically increased. This explains why the LO-phonon population peaks at the resonant tunneling voltage. A similar argument can be used to explain the maximum of the anti-Stokes line at the LO-phonon-assisted tunneling voltage.

In conclusion, we have observed a *nonlinear* behavior of nonequilibrium LO-phonon population in strongly coupled GaAs-AlAs superlattices under bias. The field dependence of the population correlates with the tunneling resonances of the conduction-band electrons. At resonant tunneling voltages, most of the hot electrons with energies below $\hbar\omega_{\mathrm{LO}}$ can transit to the neighboring well before relaxation by acoustical-phonon emission takes place. Our results suggest that hot electron cooling via acoustical-phonon emission is suppressed at the resonant tunneling condition and plays a more important role for electric fields corresponding to nonresonant condition.

We would like to thank A. Fischer for sample growth. We acknowledge helpful discussions with P. Y. Yu and R. Merlin. This work was supported in part by the BMBF of the Federal Republic of Germany.

[1] L. Esaki and R. Tsu, IBM J. Res. Dev. **14**, 61 (1970).
[2] F. Capasso, K. Mohammed, and A. Y. Cho, IEEE J. Quantum Electron. **QE-22**, 1853 (1986).
[3] See, e.g., J. Shah, *Hot Carriers in Semiconductor Nanostructures: Physics and Applications* (Academic, Boston, 1992).
[4] W. Pötz and P. Kocevar, Phys. Rev. B **28**, 7040 (1983).
[5] D. von der Linde, J. Kuhl, and H. Klingenberg, Phys. Rev. Lett. **44**, 1505 (1980).
[6] C. L. Collins and P. Y. Yu, Phys. Rev. B **30**, 4501 (1984).
[7] J. A. Kash, J. C. Tsang, and J. M. Hvam, Phys. Rev. Lett. **54**, 2151 (1985).
[8] M. C. Tatham, J. F. Ryan, and C. T. Foxon, Phys. Rev. Lett. **63**, 1637 (1989).
[9] K. T. Tsen, K. R. Wald, T. Ruf, P. Y. Yu, and H. Morkoç, Phys. Rev. Lett. **67**, 2557 (1991).
[10] D. Y. Oberli, G. Böhm, and G. Weimann, Phys. Rev. B **47**, 7630 (1993).
[11] P. Brockmann, J. F. Young, P. Hawrylak, and H. M. van Driel, Phys. Rev. B **48**, 11 423 (1993).
[12] D. S. Kim, A. Bowholkha, J. M. Jacob, J. J. Song, J. F. Klem, H. Hou, C. W. Tu, and H. Morkoç, Phys. Rev. B **51**, 5449 (1995).
[13] H. Schneider, K. von Klitzing, and K. Ploog, Europhys. Lett. **8**, 575 (1989).
[14] W. Müller, H. T. Grahn, K. von Klitzing, and K. Ploog, Phys. Rev. B **48**, 11 176 (1993).
[15] C. Tejedor, J. M. Calleja, L. Brey, L. Viña, E. E. Mendez, W. I. Wang, M. Staines, and M. Cardona, Phys. Rev. B **36**, 6054 (1987).
[16] V. J. Goldman, D. C. Tsui, and J. E. Cunningham, Phys. Rev. B **36**, 7635 (1987).
[17] W. Müller, H. T. Grahn, K. von Klitzing, and K. Ploog, Phys. Rev. B **50**, 10 998 (1994).
[18] Due to the $1/Q^2$ dependence in the Fröhlich matrix element, the intersubband scattering rate is very large if the subband spacing is close to $\hbar\omega_{\mathrm{LO}}$. For a subband spacing $\gg\hbar\omega_{\mathrm{LO}}$, the Q involved is large and one might need to consider the effect of deformation potential interaction.
[19] D. Gammon, R. Merlin, and H. Morkoç, Phys. Rev. B **35**, 2552 (1987).
[20] T. Ruf, V. I. Belitsky, J. Spitzer, V. F. Sapega, M. Cardona, and K. Ploog, Phys. Rev. Lett. **71**, 3035 (1993).
[21] Z. P. Su, T. Ruf, K. R. Wald, P. Y. Yu, and K. T. Chan, *Proceedings of the 22nd International Conference on the Physics of Semiconductors,* edited by D. J. Lockwood (World Scientific, Singapore, 1995), p. 963.
[22] D. Y. Oberli, D. R. Wake, M. V. Klein, J. Klem, T. Henderson, and H. Morko¢, Phys. Rev. Lett. **59**, 696 (1987).
[23] See, e.g., M. Asche and O. G. Sarbei, Phys. Status Solidi B **126**, 607 (1984).